

B, V, I – photometry of 20 dwarf irregular galaxies within 10 Mpc

L. Makarova,^{1,2} * I. Karachentsev,¹ L. Rizzi,³ R. B. Tully,⁴ G. Korotkova¹

¹Special Astrophysical Observatory, Nizhnij Arkhyz, Karachaevo-Cherkessia, Russia 369167

²Isaac Newton Institute of Chile, SAO Branch

³Joint Astronomy Centre, 660 N. A’ohoku Place, University Park, Hilo, HI 96720, USA

⁴Institute for Astronomy, University of Hawaii, 2680 Woodlawn Drive, Honolulu, HI 96822, USA

8 November 2018

ABSTRACT

CCD – photometry is presented for 20 dIrr galaxies situated in the nearby complexes CenA/M83, and CVnI as well as in the general field of the Local Volume. We present integrated magnitudes of the galaxies in B, V, I - bands and also surface brightness profiles to a median isophote $\mu_B \sim 28$ mag sq. arcsec⁻¹. The popular Sersic parameterization of surface brightness profiles generally does a poor job of simultaneously fitting the inner cores and outer exponential surface brightness fall-offs observed in many of our targets. The observed sample is a part of a general project to image about 500 nearby ($D < 10$ Mpc) dwarf galaxies in multiple bands.

Key words: galaxies: dwarf — galaxies: photometry — galaxies: fundamental parameters — galaxies: irregular

1 INTRODUCTION

Dwarf galaxies in the Local Volume ($D \leq 10$ Mpc) are well recognised now as important objects for our understanding of such diverse topics as star formation, galaxy evolution, and large scale structure. Many nearby galaxies are well resolved into individual stars, which gives a possibility to estimate their distances via the luminosity of the tip of Red Giant Branch (TRGB). The study of the nearby universe allows us to probe the cosmic structure and galaxy properties at the present epoch and thus serves as a reference for evolutionary studies. Recent systematic surveys for dwarf galaxies have doubled the number of objects known in the Local Volume (=LV) which are collected in the Catalogue of Neighbouring Galaxies (=CNG, Karachentsev et al. (2004)). **Recent discoveries (see, for example, Belokurov et al. (2006), Kuposov et al. (2008)) also increase extremely the number of known dwarf galaxies in our Local group.** Unfortunately, the discovery of large numbers of nearby galaxies, mostly of low surface brightness, has not been accompanied by systematic photometric studies. As a result, many new members of the LV so far have only rough estimates of their apparent magnitudes. There is no homogeneous optical survey embracing galaxies of both northern and southern hemispheres. The uniform survey 2MASS was performed in the near infrared bands (Jarrett et al. (2000)). However, it was insensitive to objects of low surface bright-

ness because of short exposure times and high sky backgrounds. Most LV galaxies are not represented in 2MASS. **About 65% of our sample galaxies are presented in the SDSS, but the exposures are too short to analyze the low surface brightness objects.** At present we are faced with the strange situation that the majority of the LV galaxies have radial velocities measured with $\sim 1\%$ accuracy and distances determined with an error $\sim 10\%$, but the integrated magnitudes of many nearby galaxies have uncertainties of 0.5 mag. This discordance makes it difficult to study the faint end of the luminosity function in detail. The main photometric parameters, such as total magnitudes and colours, remain poorly known for many nearby dwarf galaxies. A study of these galaxies not only in visual bands (B and V Johnson-Cousins filters), but also in the near infrared (I Cousins filter), where extinction is less, can make it possible to investigate in detail the galaxy morphology and structure of these galaxies.

This is the fourth paper in a series of articles that present results from the observations of nearby dwarf galaxies, including presentation of their general photometric parameters. In the previous papers (Makarova (1999), Makarova et al. (2002), (2005)) we described photometry of 78 nearby galaxies. Here we present photometric data for 20 more dwarf galaxies observed with the University of Hawaii 2.2m telescope.

* email lidia@sao.ru

Table 1. General parameters of the sample

Name	Leda No.	RA	Dec	D arcmin	A_B	V_h km s ⁻¹	V_{LG} km s ⁻¹	Dist. Mpc	Method
KKH 46	2807128	09 08 36.6	+05 17 32	0.7	0.20	598	409	6	CNG, h
D634-03	2806961	09 08 53.5	+14 34 55	0.4	0.16	319	173	9.5	[1], trgb
Antlia	029194	10 04 04.0	-27 19 55	2.0	0.34	362	66	1.3	[2], trgb
KKH 60	2807134	10 15 59.4	+06 48 17	0.8	0.09	290:	–	–	–
UGC 5672	30818	10 28 20.9	+22 34 17	1.8	0.10	531	428	6	CNG, bs
KKs44	36014	11 37 53.2	-39 13 13	1.4	0.62	654	362	6.1	[3], trgb
KK 144	166137	12 25 27.9	+28 28 57	1.5	0.11	483	453	6	CNG, h
KK 149	41093	12 28 52.3	+42 10 40	0.8	0.11	407	446	6	CNG, h
KK 151	41314	12 30 23.8	+42 54 05	1.2	0.08	436	479	7	CNG, h
KK 160	166142	12 43 57.4	+43 39 41	0.8	0.11	293	346	5	CNG, h
ESO 381-018	42936	12 44 42.7	-35 58 00	1.2	0.27	610	353	5.3	[3], trgb
ESO 381-020	43048	12 46 00.4	-33 50 17	3.0	0.28	585	332	5.4	[3], trgb
KKSG 37	3097714	12 48 01.0	-12 39 22	0.6	0.22	84:	–	–	–
ESO 443-09	43978	12 54 53.6	-28 20 27	0.8	0.28	645	410	5.5	[3], trgb
DDO 155	44491	12 58 40.4	+14 13 03	1.1	0.11	214	136	2.1	CNG, trgb
PGC 45628	45628	13 09 36.6	-27 08 26	0.6	0.33	693	470	6	CNG, h
PGC 170257	170257	13 29 21.0	-21 10 45	0.6	0.46	650	457	6	CNG, h
UGC 8651	48332	13 39 53.8	+40 44 21	2.3	0.03	202	272	3.0	[2], trgb
UGC 8760	49158	13 50 51.1	+38 01 16	2.2	0.07	191	257	3.2	[2], trgb
UGC 8833	49452	13 54 48.7	+35 50 15	0.9	0.05	226	285	3.2	[2], trgb

[1] Karachentsev et al. 2006

[2] Tully et al. 2006

[3] Karachentsev et al. 2007

2 OBSERVATIONS

The galaxies were selected from the CNG in accordance with the observation season. About 2/3 of the galaxies turn out to be members of two nearby complexes: CenA/M83 group and Canes Venatici I cloud, the remaining ones lie in the general field. Some basic parameters of the sample galaxies are presented in Table 1. The columns are:

Column 1: galaxy name.

Column 2: LEDA number.

Column 3 and 4: Right ascension and Declination (2000).

Column 5: Major angular diameter from the CNG in arcminutes.

Column 6: galactic absorption in B band taken from IRAS/DIRBE maps (Schlegel, Finkbeiner, Davis (1998)). Galactic absorption in V and I can be computed as follow: $A_V = 0.768A_B$ and $A_I = 0.449A_B$.

Column 7: heliocentric radial velocity in km s⁻¹.

Column 8: The Local Group centroid radial velocity

Column 9: galaxy distance in Mpc.

Column 10: source of the distance and method of its estimation: h – radial velocity; trgb – tip of the red giant branch; bs – brightest supergiants.

Our targets were observed using the 2.2m University of Hawaii telescope at Mauna Kea Observatory, Hawaii, USA on February 17–22, 2004. We carried out direct imaging of the galaxies using the Optic CCD Camera, which gives a 9.3'×9.3' field of view with the pixel scale of 0.14"/pix. The galaxy images were obtained using B , V and I Johnson-Cousins filters with typical exposure time of 1200 sec, 900 sec and 600 sec, respectively. Bias frames, twilight flats and standard fields from Landolt (1992) were observed each night for the calibration.

3 DATA REDUCTION

3.1 Initial processing

The images were processed using the *ccdproc* package within IRAF. Initial processing of the data contained usual steps such as bias and dark frame subtraction and flat-fielding. Further reductions were made with the MIDAS package developed by ESO. Cosmic ray hits were removed with the FILTER/COSMIC procedure. The galaxy images obtained in the same filter were then co-added. The resulting B -band images of the galaxies under study are presented in Fig. 1. The picture size is 3.5'×3.5', North is up and East is left.

3.2 Sky background determination

Background stars were removed from the frames by fitting a second-degree surface in circular pixel-area. The sky background was then approximated by a tilted plane, created from a two-dimension polynomial, using the least-squares method (FIT/FLAT_SKY). The accuracy of the sky background determination is about 0.6 – 1.0 % of the original sky level. A typical value of the sky surface brightness is near 23 mag sq.sec⁻¹ in B band. Therefore, the mean error of sky determination does not exceed 0.14 – 0.23 mag.

3.3 Photometric calibration

To transform the instrumental magnitudes to the standard Johnson-Cousins system, zero points and colour coefficients were determined from the standard stars observed in the clear photometric nights at February 17, 18 and 20. We used the mean Mauna Kea summit extinction coefficients for the transformation due to nonstable result of these coefficient

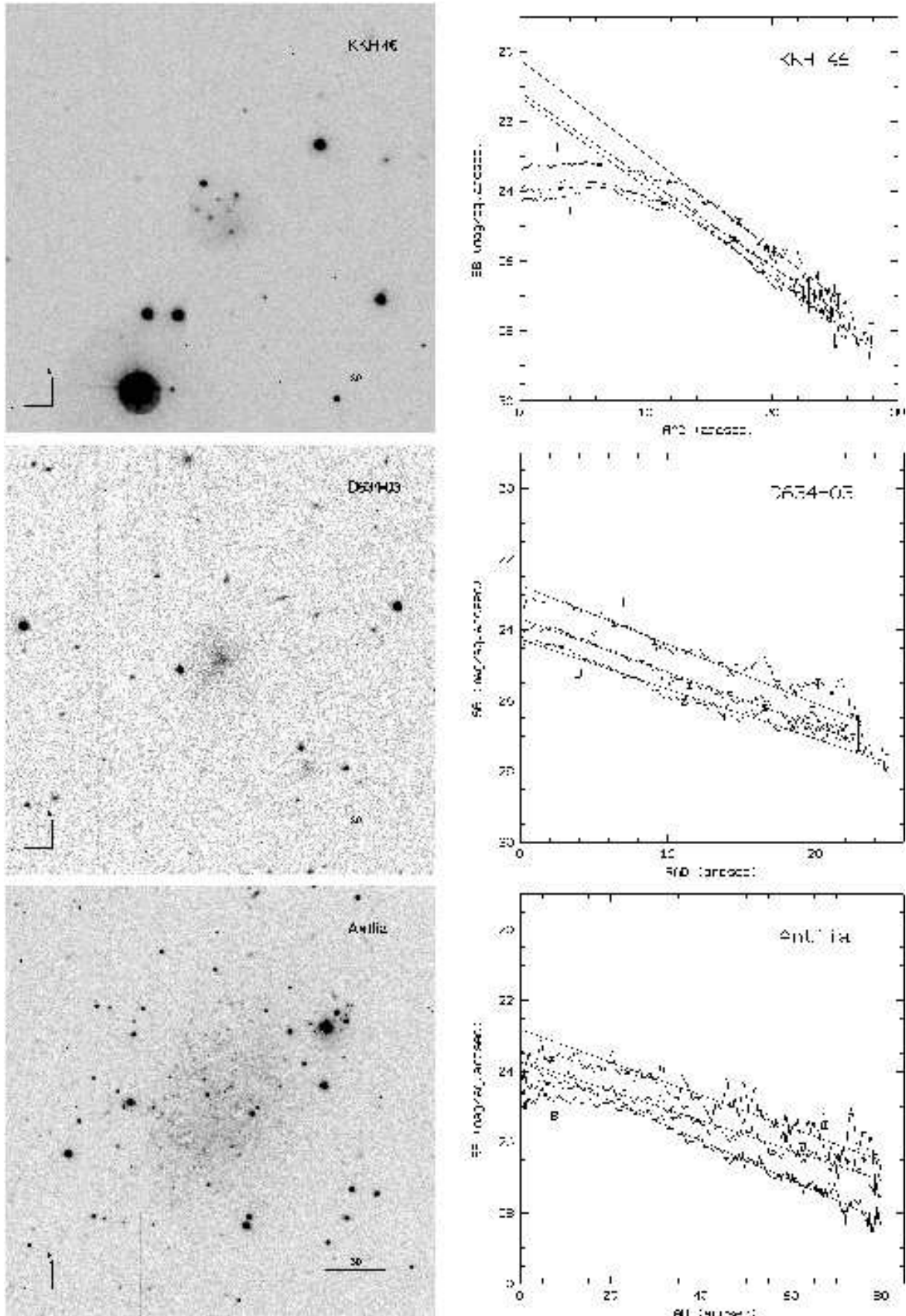


Figure 1. B-band images and B, V, I surface brightness profiles of the galaxies under study. The picture sizes are $3.5' \times 3.5'$, North is up and East is left.

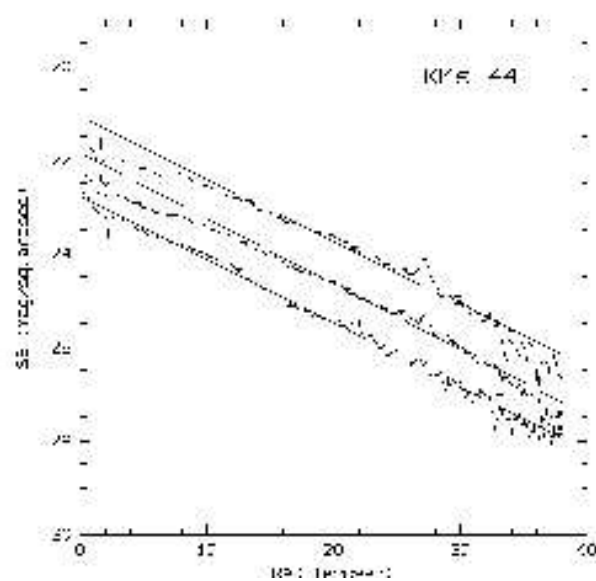
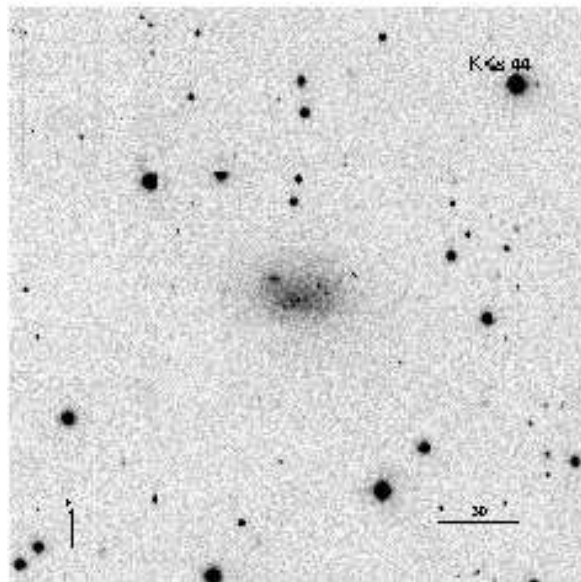
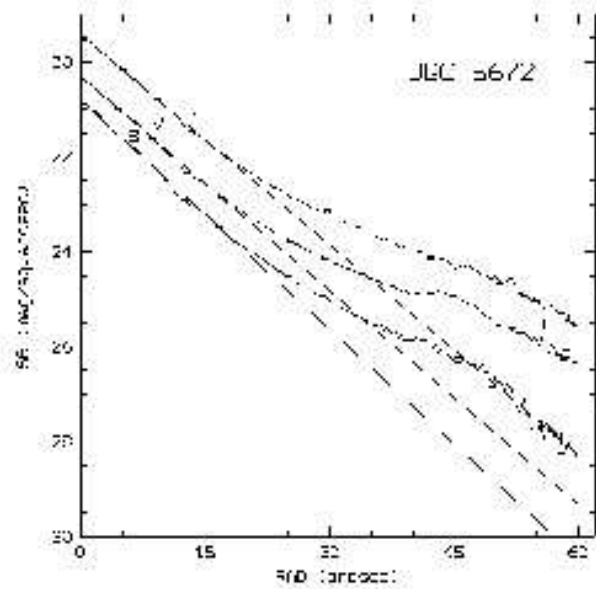
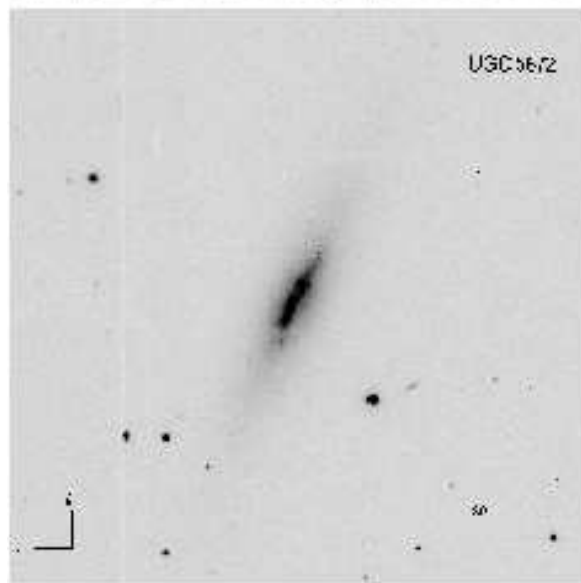
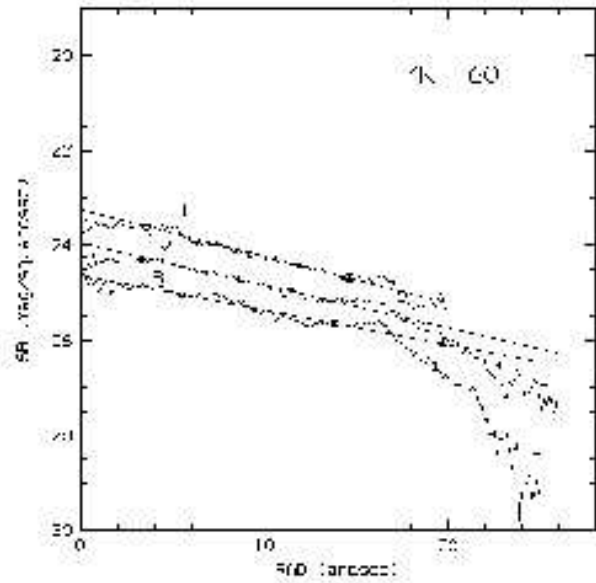
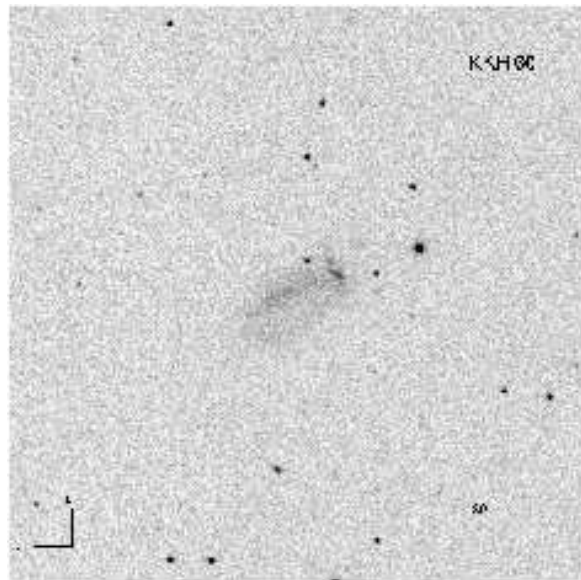


Figure 1. continued.

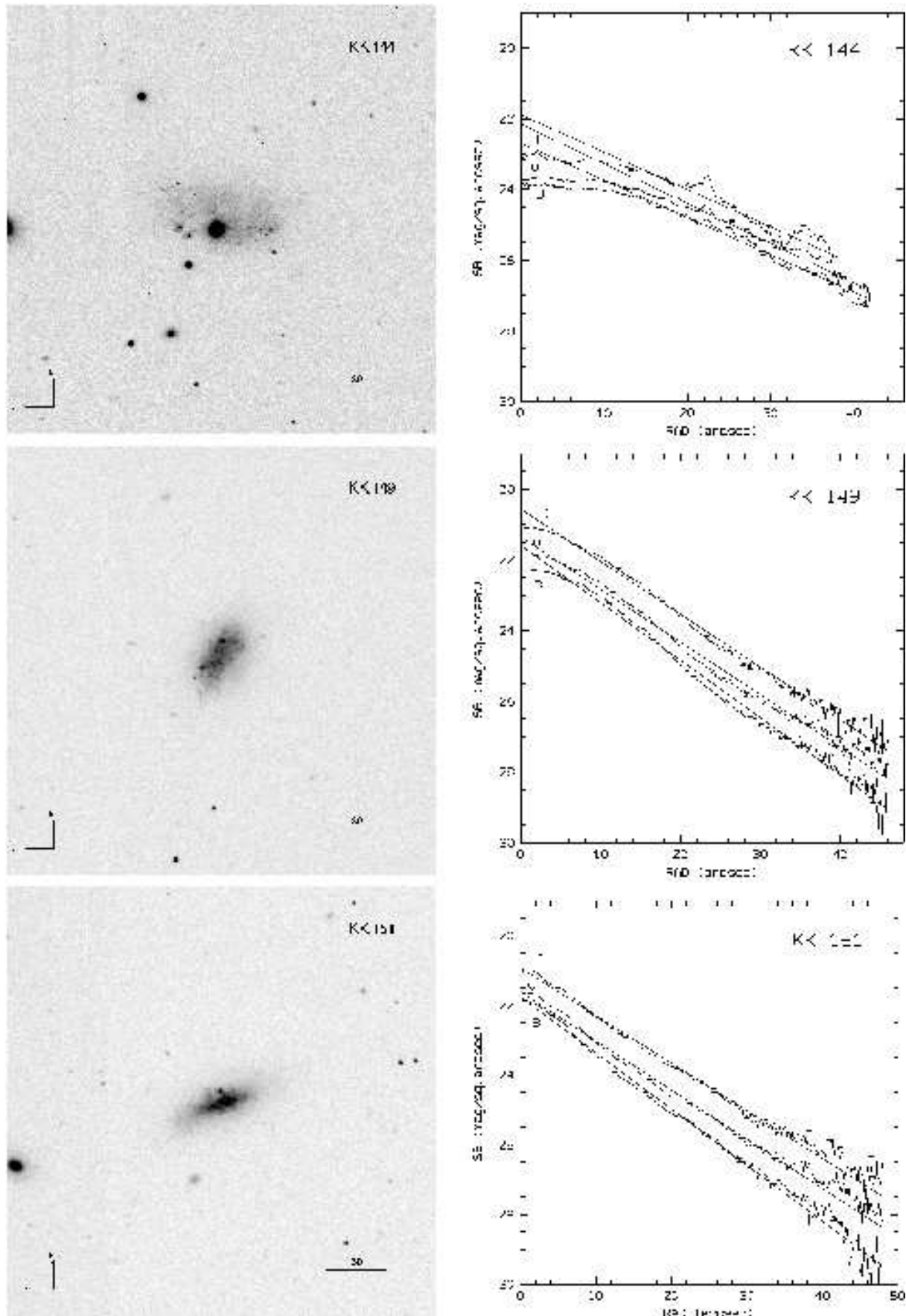


Figure 1. continued.

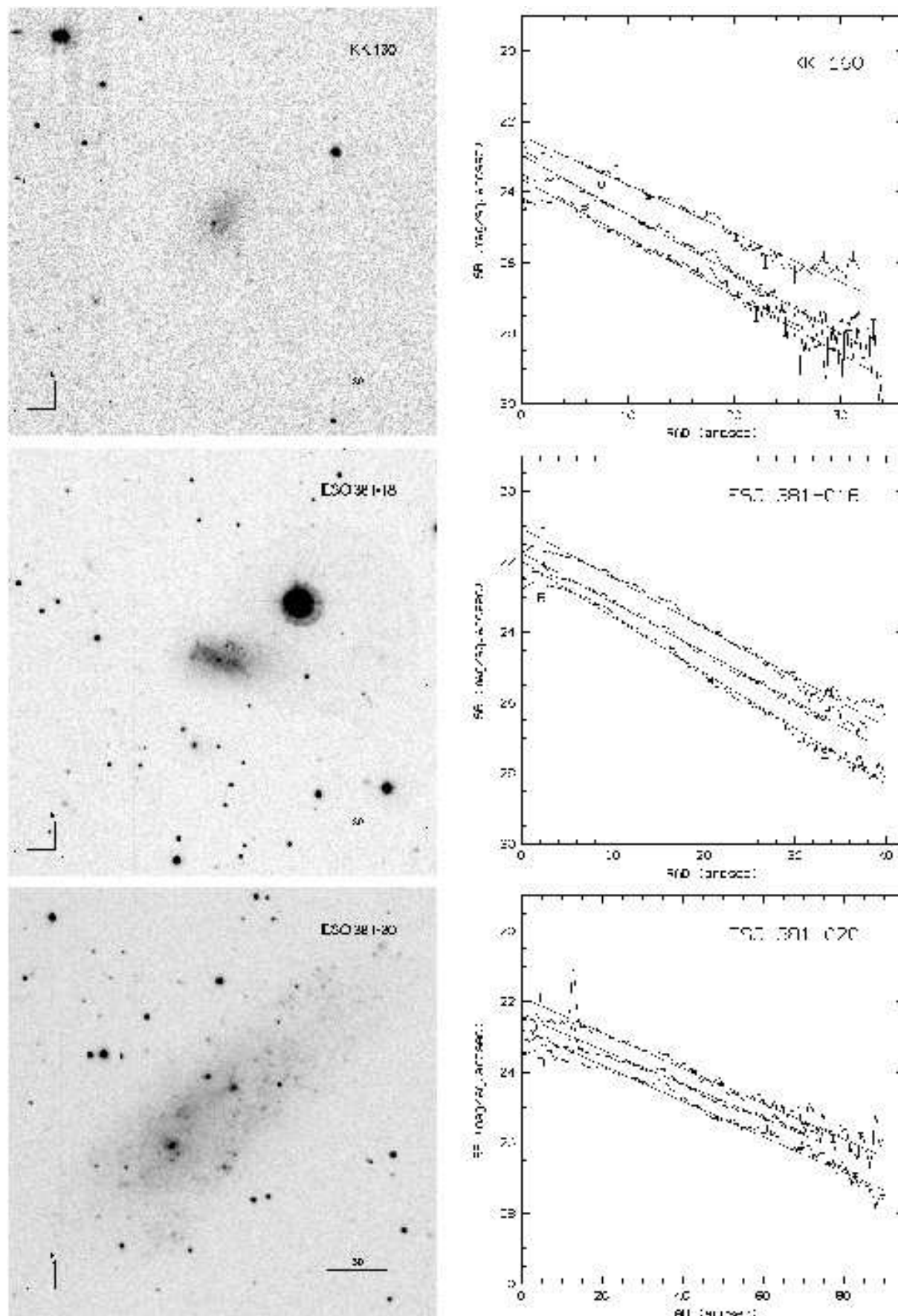


Figure 1. continued.

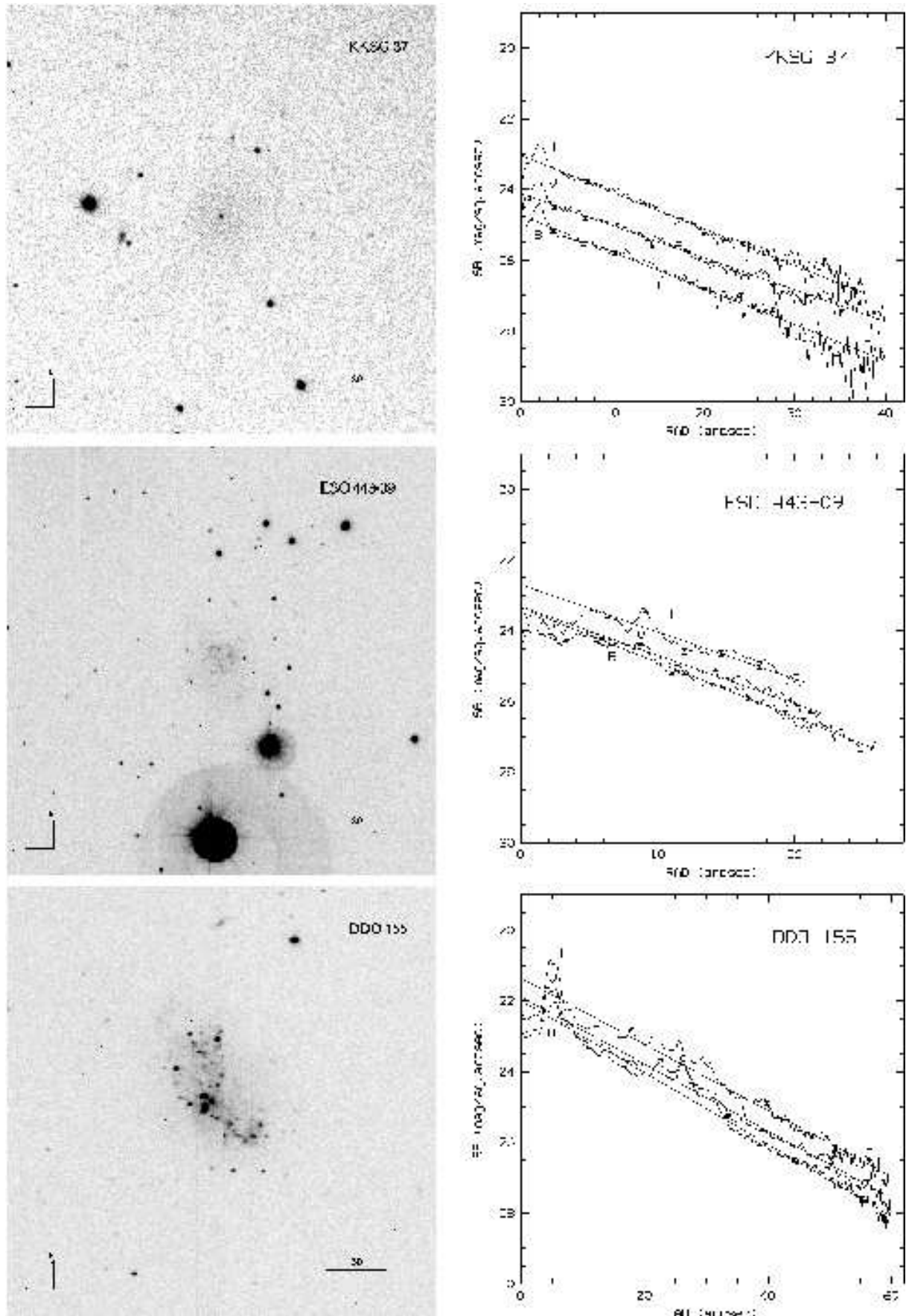


Figure 1. continued.

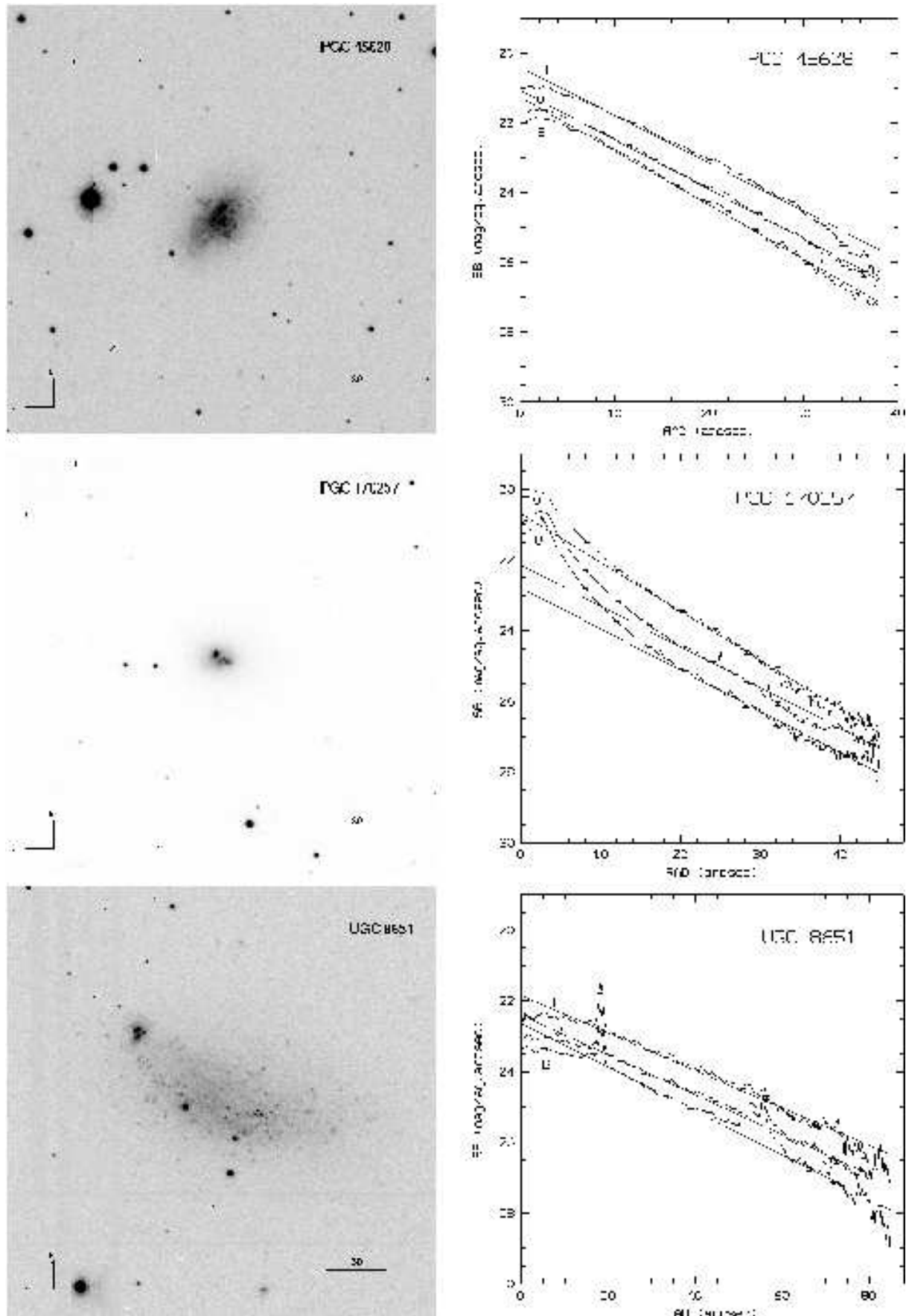


Figure 1. continued.

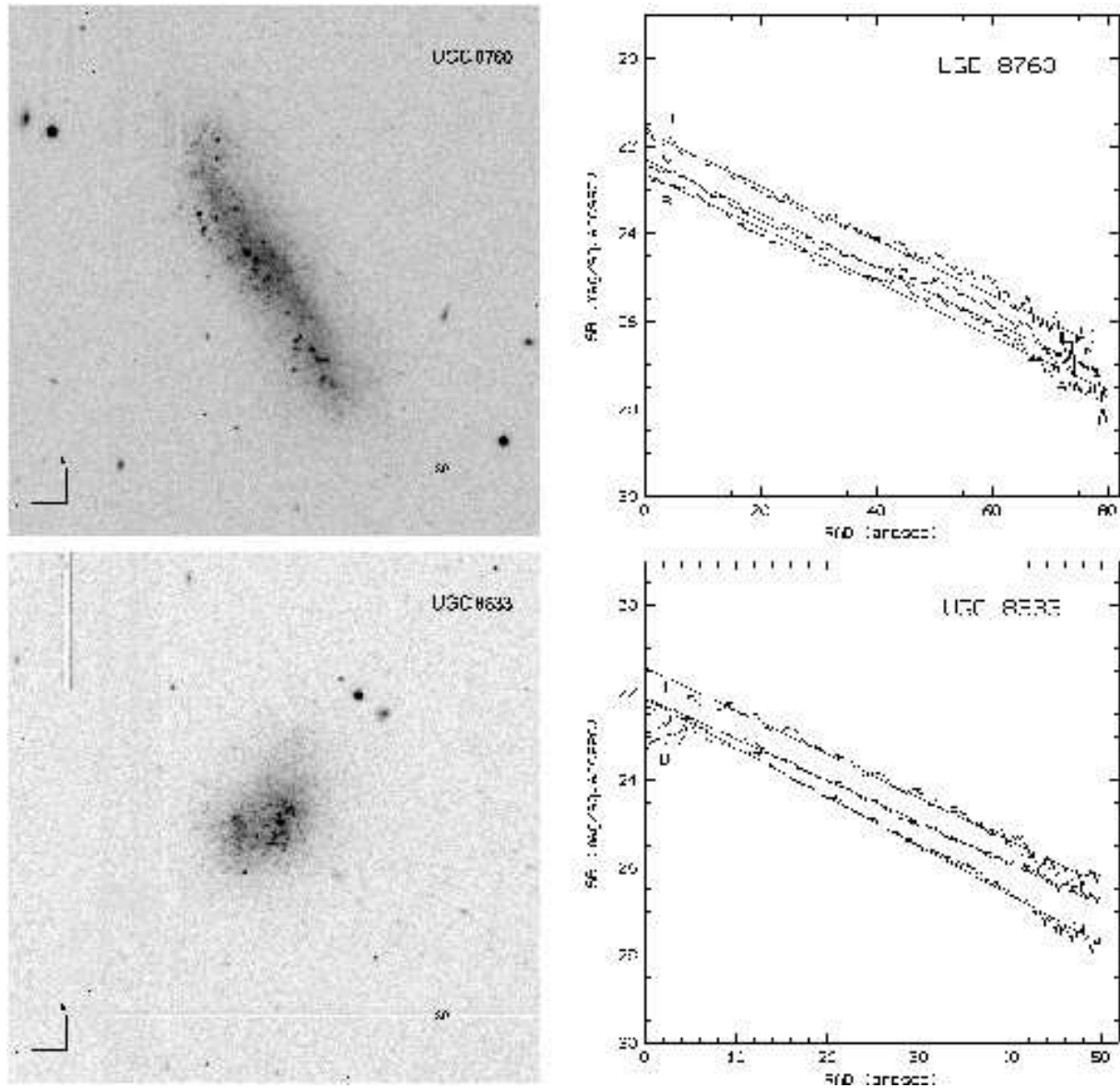


Figure 1. continued.

measurements from our data. Too few stars were observed to constrain such measurements. The observational nights at February 21 and 22 were partially non photometric. Therefore, we used zero points obtained from the appropriate standard field closest to the time of the respective observations. These zero points have good agreement, the additional uncertainty in the calibration will not exceed 0.03 mag in B , and 0.02 mag in V and I . The uncertainty of the overall transformation to the standard system is 0.01 mag in the B , V and I filters.

4 PHOTOMETRIC MEASUREMENTS

4.1 Total magnitudes

To measure total galaxy magnitudes in each band, integrated photometry was performed in circular apertures with

increasing radii from a pre-chosen centre to the faint outskirts of the galaxies. **The centers were determined interactively, because a significant part of the sample consists of the galaxies of irregular morphology.** The total magnitude was then estimated as the asymptotic value of the obtained radial growth curve. The uncertainties of the total magnitude determination were 0.05 mag in B , 0.05 mag in V and 0.08 mag in I . The measurement results are summarised in Table 2, where the columns are:

Column 1: galaxy name.

Column 2, 3 and 4: total magnitudes in B , V and I band, respectively (not corrected for galactic absorption).

Column 5 and 6: total colour $B - V$ and $V - I$, respectively (not corrected for galactic absorption).

Column 7: the standard diameter (arcsec) at the surface brightness level of 25 mag sq. sec⁻¹ in B band.

Column 8: the Holmberg diameter (arcsec) corresponding to the blue surface brightness of 26.5 mag sq. sec⁻¹.

Table 2. Total magnitudes of the dwarf galaxies

Name	B_T mag	V_T mag	I_T mag	$B - V$ mag	$V - I$ mag	D_{25} arcsec	D_{Holm} arcsec	B_{Holm} mag	M_B mag
KKH 46	16.96	16.72	16.27	0.24	0.45	28.8	41.2	16.97	-12.02
D634-03	18.27	17.78	16.92	0.49	0.86	11.0	28.8	18.45	-11.77
Antlia	15.57	15.16	14.60	0.41	0.56	47.6	92.6	15.70	-10.37
KKH 60	17.76	17.24	16.64	0.52	0.60	12.0	28.4	17.90	-
UGC 5672	14.48	13.69	12.79	0.79	0.90	60.0	98.0	14.52	-14.62
KKs44	16.30	15.74	14.71	0.56	1.03	32.6	57.0	16.34	-13.24
KK 144	15.86	15.53	14.96	0.33	0.57	46.0	72.4	15.91	-13.25
KK 149	15.54	15.04	14.31	0.50	0.73	40.0	55.0	15.59	-13.53
KK 151	15.63	15.16	14.49	0.47	0.67	38.8	60.0	15.71	-13.58
KK 160	17.65	17.02	16.10	0.63	0.92	14.8	36.2	17.87	-10.87
ESO 381-018	15.73	15.30	14.67	0.43	0.63	39.0	68.4	15.73	-13.17
ESO 381-20	14.24	13.93	13.32	0.31	0.61	90.0	150.0	14.28	-14.72
KKSG 37	18.58	17.78	16.77	0.80	1.01	6.0	30.0	18.58	-
ESO 443-09	17.38	17.17	16.52	0.21	0.65	20.4	39.4	17.45	-11.60
DDO 155	14.79	14.50	14.02	0.29	0.48	64.0	92.4	14.84	-11.93
PGC 45628	15.11	14.71	14.05	0.40	0.66	47.6	62.4	15.12	-14.28
PGC 170257	15.32	14.74	14.04	0.58	0.70	37.6	60.0	15.34	-14.14
UGC 8651	14.22	13.95	13.34	0.27	0.61	88.0	150.0	14.26	-13.20
UGC 8760	14.47	14.23	13.67	0.24	0.56	84.0	130.0	14.51	-13.11
UGC 8833	15.30	14.97	14.38	0.33	0.59	51.2	77.6	15.38	-12.27

Column 9: B magnitude within the Holmberg diameter

Column 10: absolute B total magnitude corrected for Galactic absorption.

Slight changes of a slope in about 75% of the surface brightness profiles can indicate redder colour index of the galaxies in their outer parts. This gradient occurs probably due to increase in the average age of the stellar population towards the edge of the galaxy.

4.2 Surface brightness profiles

Azimuthally averaged surface brightness profiles have been widely used (Karachentseva et al. (1996), Papaderos et al. (1996), Bremnes, Binggeli, Prugniel (1998), Gil de Paz & Madore (2005)) for the investigation of dwarf galaxies. They allow one to improve the accuracy of surface photometry in galaxies of low surface brightness and irregular structure. Azimuthally averaged surface brightness profiles for our galaxies were obtained by differentiating the galaxy growth curves with respect to radius (Bremnes et al. (1998)). The resulting profiles in the B , V and I colours are displayed in Fig. 1. Most of the galaxies were measured up to the level of 28 mag arcsec⁻² in the B filter. Mean uncertainties of the measurements were estimated by intercomparison of individual profiles for the same objects obtained from different frames in the same passband. They amount to about 0.08 mag at the 23 mag arcsec⁻² isophotal level and about 0.3 mag to 0.4 mag at the 27 mag arcsec⁻² isophotal level in each of the filters.

It is well known that surface brightness profiles of dwarf galaxies (both irregular and spheroidal) and also disks of spiral galaxies can be fitted by an exponential intensity law of brightness distribution (de Vaucouleurs (1959))

$$I(r) = I_0 * \exp(-r/h)$$

or, in magnitudes per sq.sec

$$\mu(r) = \mu_0 + 1.086 * (r/h),$$

where μ_0 is the central surface brightness and h is the exponential scale length. Most of the measured galaxies are well-fitted by an exponential law in the whole profile or in its outer parts. As can be seen from Fig. 1, most of the surface brightness profiles have a linear outer part, which can be considered as evidence for the presence of an underlying stellar disk component of the galaxy. About 70% of the surface brightness profiles show central light depression, which is very common for dwarf irregular galaxies. We also have five profiles in our sample that seem purely exponential, and two of the galaxies have prominent light excesses in their central parts. Our previous sample of nearby dwarfs (Makarova et al. (2005)) show similar tendencies.

The **unweighted** exponential fits to the surface brightness profiles were done by linear regression. The rms deviation of the derived model profiles from the original ones does not exceed 0.10 mag. The results of the fitting are presented in Table 3. The columns are:

Column 1: galaxy name.

Column 2: central surface brightness in B filter estimated from the original profile.

Column 3 and 4: best-fitting parameters of the exponential disk in B filter (the central surface brightness μ_0 (mag sq.sec⁻¹) and exponential scale length h (arcsec)).

Column 5: central surface brightness in V filter estimated from the original profile.

Column 6 and 7: best-fitting parameters of the exponential disk in V filter.

Column 8: central surface brightness in I filter estimated from the original profile.

Column 9 and 10: best-fitting parameters of the exponential disk in I filter.

Table 3. The fitting parameters of the dwarf galaxies

name	μ_B^p mag sq.sec ⁻¹	μ_B^f mag sq.sec ⁻¹	h_B arcsec	μ_V^p mag sq.sec ⁻¹	μ_V^f mag sq.sec ⁻¹	h_V arcsec	μ_I^p mag sq.sec ⁻¹	μ_I^f mag sq.sec ⁻¹	h_I arcsec
KKH 46	24.2	21.30	4.2	23.8	21.15	4.3	23.3	20.23	4.0
D634-03	24.2	24.27	7.8	23.9	23.68	7.1	23.2	22.74	6.5
Antlia	24.8	23.73	19.4	24.3	23.71	25.8	23.7	22.82	23.4
KKH 60	24.7	24.64	14.9	24.4	23.96	12.2	23.6	23.25	11.1
UGC 5672	20.8	20.81	6.8	20.3	20.31	7.2	19.5	19.44	7.4
KKs 44	22.6	22.77	8.0	22.3	21.86	7.7	21.7	21.08	8.1
KK 144	23.9	22.69	10.3	23.7	22.15	9.6	23.1	21.89	10.3
KK 149	22.3	21.60	6.7	21.8	21.35	7.3	21.1	20.56	7.3
KK 151	22.0	21.76	6.7	21.7	21.62	7.7	21.1	20.93	7.9
KK 160	24.3	23.65	6.6	23.6	22.96	6.4	22.6	22.42	7.9
ESO 381-18	22.6	21.99	6.9	22.3	21.76	7.7	21.6	21.05	7.7
ESO 381-20	23.1	22.79	21.4	23.0	22.41	22.5	22.5	21.88	21.6
KKSG 37	24.7	24.74	10.6	24.2	24.12	12.0	23.4	23.04	10.5
ESO 443-09	24.0	23.36	7.0	24.1	23.33	7.9	23.5	22.71	8.2
DDO 155	22.9	21.99	10.7	22.6	21.89	11.4	22.3	21.36	11.6
PGC 45628	21.9	21.26	7.0	21.6	21.07	7.6	21.0	20.41	7.9
PGC 170257	20.9	22.79	9.3	20.6	22.15	9.4	20.2	20.69	7.8
UGC 8651	23.3	22.63	17.5	23.1	22.40	19.3	22.4	21.85	20.5
UGC 8760	22.8	22.64	17.5	22.4	22.31	17.6	21.8	21.68	17.5
UGC 8833	23.0	22.15	9.7	22.8	22.12	11.5	22.2	21.43	11.0

The listed surface brightnesses were not corrected for the Galactic absorption.

4.3 Photometric uncertainties

Summing up all internal errors given above, we obtain the resulting errors of the total magnitude estimation to be about 0.24^m in B , V and I band, and the resulting errors of surface brightness estimation to be about 0.24^m at the 23 mag sq.sec⁻¹ isophotal level and about 0.38-0.46 at the 27 mag sq.sec⁻¹ isophotal level in each photometric band.

External photometric errors can be estimated by a comparison of the total magnitudes of the observed galaxies with the published magnitudes of these galaxies. The comparison of the total B -magnitudes estimated in the present work with those given in the articles of Bremnes, Binggeli, Prugniel (1999), Hopp&Schulte-Ladbeck (1995), Makarova et al. (1998) and Makarova et al. (2002) for five galaxies in common, yields the satisfactory agreement of -0.02 ± 0.15 mag. We did not consider other bands due to poor statistic (one-two published values).

5 NOTES ON INDIVIDUAL GALAXIES

KKH 46. This irregular knotty galaxy is one of the most isolated objects in the LV. The distance is estimated from its radial velocity with the Hubble constant $H = 72$ km/s/Mpc. The apparent magnitude of KKH 46 $g = 18.6$ is given in NED from Sloan DSS and it corresponds to a single blue knot only.

D634-03. Distance to the object was recently measured via the luminosity of TRGB (Karachentsev et al. (2006)).

Antlia. This is a dwarf companion to NGC 3109. Distance measurements to Antlia via TRGB were made by

Aparicio et al. (1997) and Tully et al. (2006) in fine mutual agreement.

KKH 60. This is an irregular galaxy of low surface brightness with an unreliable estimate of radial velocity, +286 km/s (Makarov, Karachentsev, Burenkov (2003)). Judging from its new radial velocity, +1670 km/s, measured at Arecibo (M. Haynes, personal communication), KKH 60 resides far beyond the LV.

KKs 44 = ESO 320-014. This dIrr galaxy is situated at the remote periphery of the CenA/M83 complex. The distance to the galaxy was recently determined from the TRGB by Karachentsev et al. (2007).

KK 144, KK 149, KK 151, and KK 160. Judging from their radial velocities, these four dIrr galaxies belong to the CVnI cloud. Three of them, apart from KK 160, are detected in the H α emission line (Kaisin & Karachentsev (2008)) testifying to active star formation in these dwarf systems.

ESO 381-018 and ESO 381-020. These are two dIrr galaxies on the outskirts of the CenA/M83 complex. Their distances were recently measured via TRGB (Karachentsev et al. (2007)).

KKSG 37. This is a dwarf system of very low surface brightness and rather uncertain type (dSph or dIrr). The reported HI emission with radial velocity of $+85 \pm 1$ km/s (Huchtmeier, Karachentsev, Karachentseva (2003)) has apparently a local Galactic origin. Judging from the measured colours $B - V = 0.82$, $V - I = 1.01$, KKSG 37 is a distant dSph system probably located in the Virgo Southern extension.

ESO 443-09 = KK 170. This dIrr galaxy situated at the outskirts of M83 group has a distance measured from TRGB (Karachentsev et al. (2007)).

DDO 155 = GR 8 = VIII Zw 222. A very nearby dIrr system seen in the stage of active star formation.

PGC 45628 and PGC 170257. Two dIrr galaxies on the

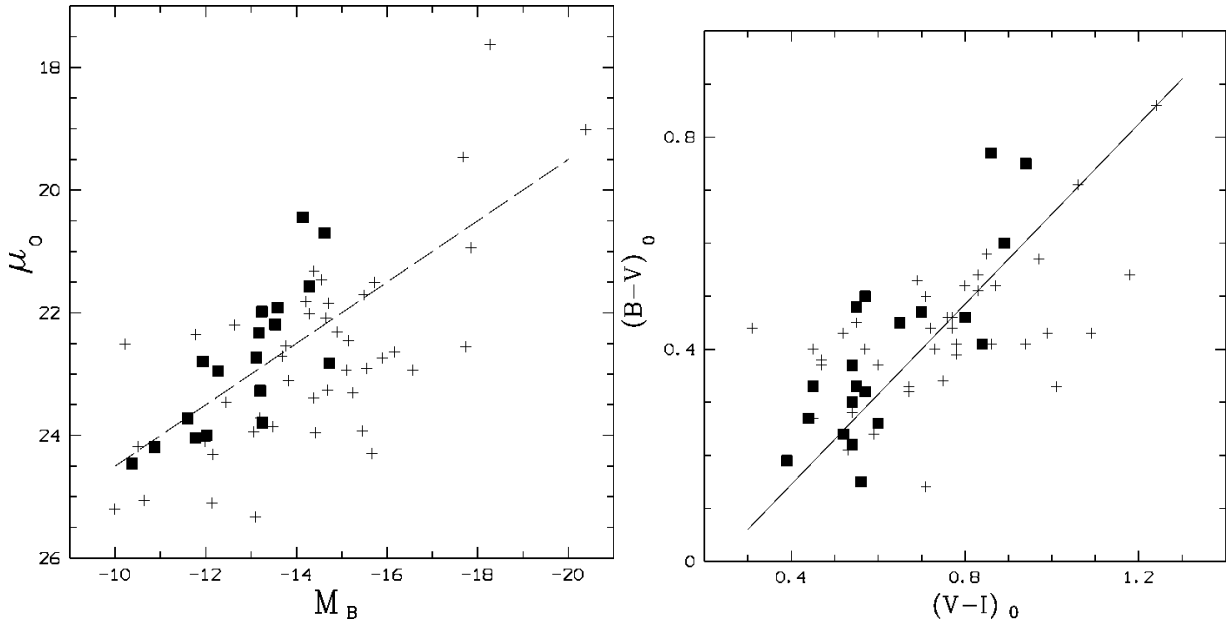


Figure 2. The distribution of central surface brightness in B filter vs. absolute B magnitude (left) and the distribution of the total colour indexes $(B - V)_0$ vs. $(V - I)_0$. All magnitudes and colour indexes are corrected for galactic absorption. The 20 dIrr galaxies from the present work are shown with filled squares. The galaxies measured in our other studies are shown with crosses.

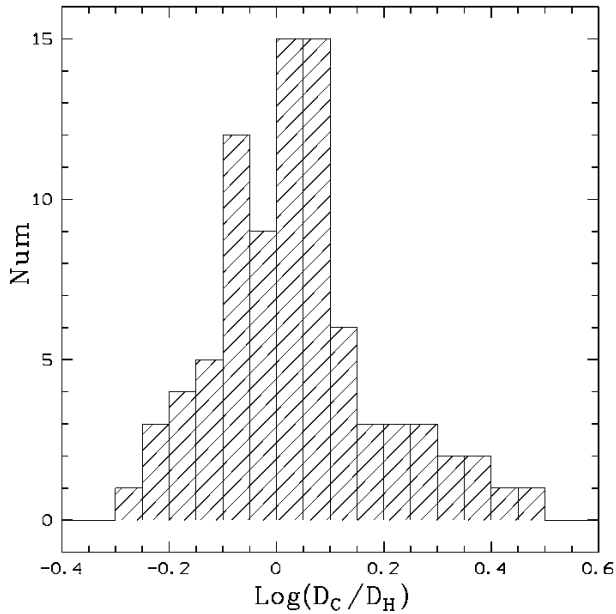


Figure 3. The distribution of nearby galaxy diameters from the Catalogue of Neighbouring Galaxies relatively to Holmberg diameters for dwarf galaxies studied by us.

periphery of the CenA/M83 complex with distances estimated from their radial velocities.

UGC 8651, UGC 8760, and UGC 8833. Three dIrr galaxies with accurate TRGB distances 3.01, 3.18, and 3.19, respectively, in a group of dwarfs on the near side of the CVnI cloud (Tully et al. (2006)). The R-band profiles of UGC 8651 and UGC 8760 were measured by Swaters (1999).

6 DISCUSSION AND CONCLUSIONS

In this work we present imaging and general photometric parameters of 20 nearby dwarf galaxies. It is seen in Table 2 and Table 3 that the blue central surface brightnesses of the 20 irregular galaxies under study lies within the range of $[20.8 - 24.8]$ mag sq. sec $^{-1}$ and their total absolute magnitudes occupy the interval of $[-10.3, -14.8]$ mag. Total parameters of these galaxies follow the common relations for dwarf galaxies. The distribution of central surface brightness and absolute magnitudes for the objects of our sample is presented in the left panel of Fig.2. In general, the galaxies follow the relation $\mu_0(B) \propto 0.5 M_B$ (dashed line) similar to the dwarf population of the Local Group (Gebel, Gallagher, Harbeck (2003)). Total colour indexes $B - V$ and $V - I$ of the galaxies under study (Fig.2, right panel) follow the relation $B - V = 0.85(V - I) - 0.2$ similar to dIrr and dSph galaxies from our previous paper (Makarova (1999)) with the scatter $\sim 0.15^m$.

The surface brightness profiles of the dwarf Irr galaxies from our sample are well-fitted by an exponential law in its outer parts, whereas in the central parts they show light depression. This tendency is very common for nearby dwarf galaxies, including dIrrs and dSphs (see, for example, the big series of nearby dwarf galaxies study by Bremnes et al. (1998); Bremnes, Binggeli, Prugniel (2000); Barazza, Binggeli, Prugniel (2001); Parodi, Barazza, Binggeli (2002)). In a number of studies of dwarf (mostly spheroidal) galaxies the central light depression of surface brightness profiles was fitted by the Sersic law $I(r) = I_0 * \exp[-(r/r_0)^n]$ (Jerjen, Binggeli, Freeman (2000), Graham & Guzman (2003)). With the Sersic index $n < 1$, surface brightnesses flatten toward a constant surface brightness core at the centre and steepen down from the exponential fall-off at large radii. One might imagine that the dwarfs would typically be tidally truncated and have a cutoff which could have a form described by Ser-

sic $n < 1$. However, most of the profiles considered by us and in the studies mentioned above are consistent with an exponential decay with radius with no hint of a cutoff. The Sersic parameterization does **not** adequately describe this characteristic of a flat core (requiring Sersic index $n < 1$) but an exponential decay at large radii as far as can be followed (described by Sersic index $n = 1$). Perhaps dwarfs that are in close proximity to a big galaxy and have had a close encounter might be tidally truncated and consequently be reasonably described by a Sersic index $n < 1$. However our dwarfs that are for the most part gas-rich and relatively isolated might have their unmodified ‘natural’ shape and that shape, evidently, is described by Sersic $n = 1$ in their outer parts.

The surface brightness profiles allow us to determine the characteristic isophotes of major diameters of galaxies in the CNG. The distribution of CNG diameters relatively to Holmberg diameters for 85 dwarf galaxies studied by us is presented in Fig.3. The diameters measured in the CNG are not homogeneous. For most bright galaxies (with NGC, UGC, ESO numbers) the diameters nearly correspond to the level of $\mu_B = 25$ mag sq sec⁻¹. Diameters of the low surface brightness objects from the KK, KKH, KKR, KKSG and KKs lists were measured at fainter isophotes. Following the data of Fig.3 we conclude that the typical diameter of a CNG galaxy is close to the Holmberg diameter, exceeding it by about 10%. The median isophote of CNG diameters corresponds to about 26.8 mag sq.sec⁻¹ in B according to our data.

Acknowledgments. This work was partially supported by RFFI grants 07-02-00005 and 08-02-00627 and grant DFG-RGBR 06-02-04017.

REFERENCES

- Aparicio A., Dalcanton J. J., Gallart C., Martinez-Delgado D., 1997, AJ, 114, 1447
 Barazza F., Binggeli B., Prugniel P., 2001, A&A 373, 12
 Belokurov V., Zucker D.B., Evans N.W. et al., 2006, ApJ, 647, L111
 Bremnes T., Binggeli B., Prugniel P., 1998, A&AS 129, 313
 Bremnes T., Binggeli B., Prugniel P., 1999, A&AS 137, 337
 Bremnes T., Binggeli B., Prugniel P., 2000, A&AS 141, 211
 De Vaucouleurs G., 1959, Handbuch der Physik, 53, 275, Flugge S.(ed.), Springer, Berlin
 Gil de Paz A., Madore B., 2005, ApJS, 156, 345
 Graham A., Guzman R., 2003, AJ, 125, 2936
 Grebel E. K., Gallagher J. III, Harbeck D., 2003, AJ, 125, 1926
 Hopp U., Schulte-Ladbeck R., 1995, A&AS, 111, 527
 Huchtmeier W.K., Karachentsev I.D., Karachentseva V.E., 2003, A&A, 401, 483
 Jarrett T.H., Chester T., Cutri R., et al., 2000, AJ, 119, 2498
 Jerjen H., Binggeli B., Freeman K.C., 2000, AJ, 119, 593
 Kaisin S.S., Karachentsev I.D., 2008, A&A, 479, 603
 Karachentseva V., Prugniel P., Vennik J., Richter G., Thuan T., Martin J., 1996, A&AS, 117, 343
 Karachentsev I., Karachentseva V., Huchtmeier W., Makarov D., 2004, AJ, 127, 2031
 Karachentsev I.D., Dolphin A., Tully R.B., et al., 2006, AJ, 131, 1361
 Karachentsev I.D., Tully R.B., Dolphin A., et al., 2007, AJ, 133, 504
 Kuposov S., Belokurov V., Evans N. W., et al., 2008, ApJ, 686, 279
 Landolt A., 1992, AJ, 104, 340
 Makarov D.I., Karachentsev I.D., Burenkov A.N., 2003, A&A, 405, 951
 Makarova L., 1999, A&AS, 139, 491
 Makarova L., Karachentsev I., Takalo L., Heinamaki P., Valtonen M., 1998, A&AS, 128, 459
 Makarova L., Karachentsev I., Grebel E., Barsunova O., 2002, A&A, 384, 72
 Makarova L., Karachentsev I., Grebel E., Harbeck D., Korotkova G., Geisler D., 2005, A&A, 433, 751
 Papaderos P., Loose H.-H., Thuan T., Fricke K., 1996, A&AS, 120, 207
 Parodi B. R., Barazza F. D., Binggeli B., 2002, A&A, 388, 29
 Schlegel D.J., Finkbeiner D.P., Davis M., 1998, ApJ, 500, 525
 Swaters R., 1999, Dark Matter in Late-type Dwarf Galaxies, Thesis, Groningen
 Tully R.B., Rizzi L., Dolphin A.E. et al., 2006, AJ, 132, 729